Inorganic Chemistry

Communication

pubs.acs.org/IC

# Magnetic Structure and Properties of the Rechargeable Battery Insertion Compound $Na_2FePO_4F$

Maxim Avdeev,*[,†] Chris D. Ling,[‡] Thiam Teck Tan,[§] Sean Li,[§] Gosuke Oyama,[∥] Atsuo Yamada,[∥,⊥] and Prabeer Barpanda[∥,⊥,#]

[†]Bragg Institute, B87, Australian Nuclear Science and Technology Organization, Locked Bag 2001, Kirrawee DC NSW 2232, Australia

[‡]School of Chemistry, The University of Sydney, Sydney NSW 2006, Australia

[§]School of Materials Science and Engineering, University of New South Wales, Kensington NSW 2052, Australia

[∥]Department of Chemical System Engineering, The University of Tokyo, Bunkyo-ku, Tokyo 113-8656, Japan

[⊥]Unit of Element Strategy Initiative for Catalysts & Batteries, ESICB, Kyoto University, Kyoto 615-8510, Japan

[#]Materials Research Center, Indian Institute of Science, C.V. Raman Avenue, Bangalore 560012, India

Supporting Information

**ABSTRACT:** The magnetic structure and properties of sodium iron fluorophosphate $Na_2FePO_4F$ (space group *Pbcn*), a cathode material for rechargeable batteries, were studied using magnetometry and neutron powder diffraction. The material, which can be described as a quasi-layered structure with zigzag Fe-octahedral chains, develops a long-range antiferromagnetic order below ~3.4 K. The magnetic structure is rationalized as a super-exchange-driven ferromagnetic ordering of chains running along the *a*-axis, coupled antiferromagnetically by super-super-exchange via phosphate groups along the *c*-axis, with ordering along the *b*-axis likely due to the contribution of dipole−dipole interactions.

Sodium-ion batteries have recently attracted significant attention because the low cost of sodium creates potential for economical large-scale energy storage.[1] However, only a handful of suitable cathode materials have been studied in detail. Inspired by $LiFePO_4$,[2] various phosphor−polyanionic systems have been explored, leading to the discovery of $Na_2FePO_4F$ fluorophosphate, which is capable of acting as a host for both Na and Li (de)insertion.[3] The material is isostructural to $Na_2CoPO_4F$[4] and $Na_2MgPO_4F$,[5] crystallizing in an orthorhombic structure (space group *Pbcn*, #60) built from face- and vertex-sharing $FeO_4F_2$ octahedra that form parallel chains bridged by $PO_4$ tetrahedra. This forms a robust framework that offers 3.5 V reversible electrochemical activity with minimal volume strain and excellent cycling life.[3,6]

In addition to its electrochemical properties, $Na_2FePO_4F$ is an intriguing system for magnetic studies. Previous ab initio DFT calculations suggested that $Na_2FePO_4F$ should be magnetically ordered, although the results were inconclusive as to whether the material is more stable in ferromagnetic (FM) or antiferromagnetic (AFM) configurations.[7] However, at the same time, Mössbauer spectroscopy measurements down to 4.2 K reported no evidence for long-range magnetic ordering.[8] In order to resolve this apparent discrepancy and as a continuation of ongoing characterization of polyanionic cathodes (ref 9 and references therein), we have now studied $Na_2FePO_4F$ using magnetometry and neutron diffraction down to 1.5 K. We have discovered that the material does indeed undergo long-range magnetic ordering into an AFM type structure. Although the magnetic ordering transition occurs at quite low temperature (~3.4 K) and so does not directly affect battery performance, this experimental clarification of the magnetic ground state is important because it will permit further DFT calculations with improved accuracy and correspondingly improved quantitative predictions of electronic and electrochemical properties. As was shown by numerous examples, including ab initio calculations for the title compound,[10] treating a magnetically ordered material as a non-spin-polarized system results in very significant errors of both crystal structural parameters and predicted intercalation voltages, reaching up to 20−30% for the latter. In this Communication, we demonstrate that $Na_2FePO_4F$ magnetically orders at low temperature and report for the first time the experimentally determined magnetic structure and properties of $Na_2FePO_4F$.

Magnetic susceptibility measured at 100 Oe as a function of temperature clearly showed a signature of an AFM transition at ~3.4 K (Figure 1, inset). No analysis of the data with the Curie−Weiss equation was possible due to the presence of a small amount of FM impurity (further confirmed by magnetization measurements as a function of magnetic field that showed an FM response up to 150 K, shown in Figure S1 of the Supporting Information). Therefore, in order to suppress impurity contributions, an additional measurement was carried out under the field of 50 kOe (Figure 1). These data were successfully analyzed in a high-temperature range (200−300 K) with the modified Curie−Weiss law $\chi = C/(T - \Theta_{CW}) + \chi_0$, where $\chi_0$ includes all temperature-independent contributions. The analysis yielded $\Theta_{CW} = -5.1(8)$ K, $\chi_0 = 0.00374$ emu/mol, and an effective moment $\mu_{eff} = 5.46(2)\ \mu_B$. The negative sign of $\Theta_{CW}$ points to predominantly antiferromagnetic interactions in the system, and the value of the effective moment suggests an

**Received:** October 4, 2013
**Published:** December 26, 2013

   dx.doi.org/10.1021/ic402513d | *Inorg. Chem.* 2014, 53, 682−684

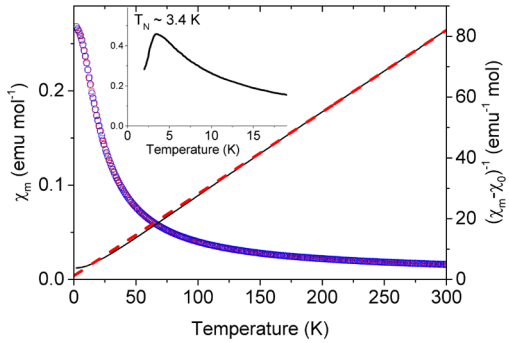


**Figure 1.** ZFC and FC (red and blue symbols, respectively) molar magnetic susceptibility $\chi_m$ and $1/(\chi_m - \chi_0)$ (black solid line) as a function of temperature for $Na_2FePO_4F$ (50 kOe). Curie–Weiss fit is shown by the red dashed line. Inset shows the susceptibility in the vicinity of the transitions (100 Oe).

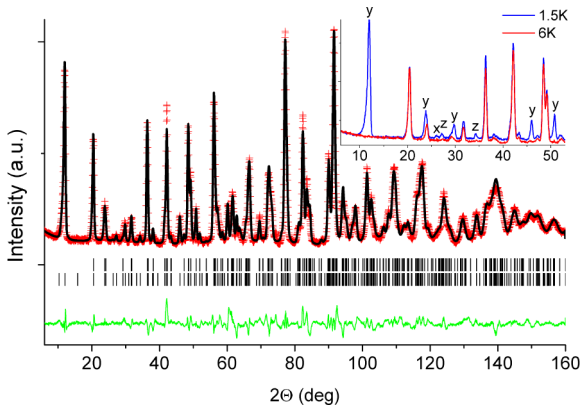


**Figure 2.** Rietveld plot for the $Na_2FePO_4F$ neutron powder diffraction data collected at 1.5 K. The red crosses and black and green solid lines indicate the observed and calculated patterns and their difference, respectively. The top and bottom tick marks indicate the position of the nuclear and magnetic diffraction peaks, respectively. $R_p$ = 4.89%, $R_{wp}$ = 6.68%, $R_F$ = 2.99%, and $R_{mag}$ = 10.6%. Inset shows the NPD data (offset for clarity) collected above (red) and below (blue) magnetic transition. The magnetic diffraction peaks corresponding to the magnetic moment components along the *a*-, *b*-, and *c*-axes are labeled *x*, *y*, and *z*, respectively.

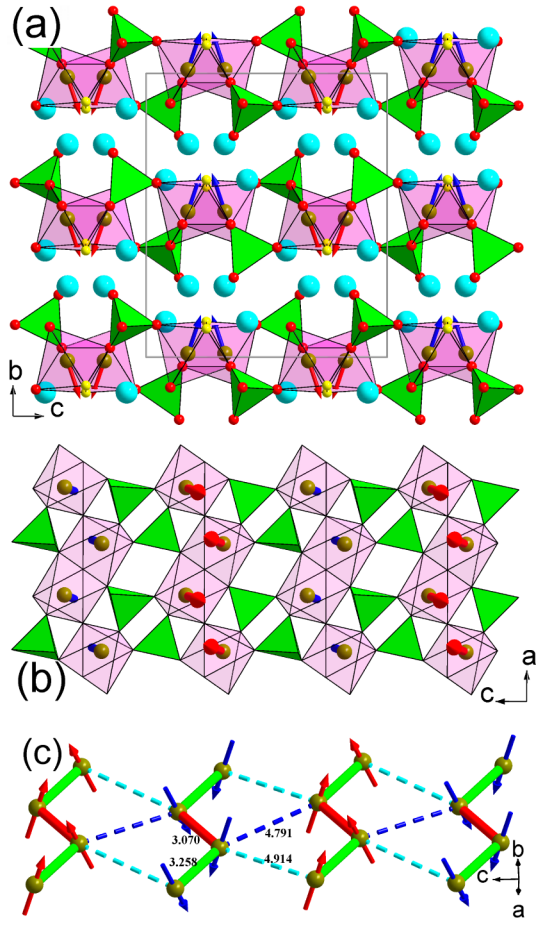


**Figure 3.** View of the crystal and magnetic structure of $Na_2FePO_4F$ along (a) and perpendicular (b) to the quasi-layers. The octahedra and tetrahedra correspond to $[FeO_4F_2]$ and $[PO_4]$ coordination polyhedra, respectively. Cyan, red, and yellow balls show Na, O, and F atoms, respectively. The shortest super- and super-super-exchange pathways are shown in (c) as solid and dashed lines, respectively, with nonequivalent distances shown in different colors.

unquenched orbital moment of ($\mu_{eff}^{L+S}(Fe^{2+})$ = 5.48 $\mu_B$), typical of the values observed in $Fe^{2+}$ compounds ( ref 11 and references therein).

Data collected at 6 K, i.e., above the transition expected from the magnetic susceptibility measurements, were successfully analyzed using the original model based on X-ray diffraction data.[3] The final Rietveld plot and crystallographic information are presented in Figure S2 and Table S1 of the Supporting Information, respectively.

Examination of the neutron diffraction patterns collected at 1.5 K revealed additional diffraction peaks due to magnetic ordering in agreement with the magnetic susceptibility data. All the diffraction peaks with a magnetic scattering contribution could be indexed by the chemical unit cell, i.e., with the propagation vector $k$ = (0,0,0). Representational analysis performed with BasIReps[12] showed that for the Fe(8d) site of the *Pbcn* space group the magnetic representation decomposes in terms of eight one-dimensional irreducible representations (IR) as $\Gamma_{mag}$ = 3Γ1 + 3Γ2 + 3Γ3 + 3Γ4 + 3Γ5 + 3Γ6 + 3Γ7 + 3Γ8. The associated basis vectors are listed in Table S3 of the Supporting Information. The best agreement between experimental and calculated NPD patterns was obtained for the Γ2 representation equivalent to the *Pb′c′n′* Shubnikov group (Opechowski–Guccione number 60.9.496). The next best model based on the IR Γ5 not only produced significantly higher $R_{mag}$ (20.8% vs 10.6% for Γ2) but also suggested ferromagnetic ordering with the moment parallel to the *b*-axis (Table S2, Supporting Information), which contradicted the susceptibility measurement. Therefore, the NPD data clearly pointed to the IR Γ2. The strongest magnetic diffraction peaks indicated that the largest magnetic moment component is along *b*-axis. However, further careful examination of the NPD data revealed that, although much weaker, peaks indicative of components along *a*- and *c*-axes are also present (Figure 2, inset). The Rietveld plot and crystallographic information are presented in Figure 2 and Table S2 of the Supporting Information, respectively. The determined value of the moment components along *a*-, *b*-, and *c*-axes are 0.44(15), 3.30(2), and 1.11(6) $\mu_B$, respectively. The total moment, 3.51(3) $\mu_B$, is slightly lower than that expected for high-spin $d^6$ S = 2 $Fe^{2+}$. However, assuming Brillouin function behavior of the magnetization and $T_N$ = 3.4 K, we obtain 3.79 $\mu_B$ as a ground state moment, which is reasonably close to the


dx.doi.org/10.1021/ic402513d | *Inorg. Chem.* 2014, 53, 682–684

theoretical spin-only value of 4 $\mu_B$.This suggests quenching of the orbital moment, although it could also be a result of the local disruption of fragile magnetic order in zigzag chains.

Analysis of crystal structure topology and geometry suggests that the magnetic sublattice can be viewed as being built of chains of face- and vertex-sharing $[FeO_4F_2]$ octahedra linked *via* phosphate groups into quasi-layers (Figure 3a-b). In agreement with the Goodenough-Kanamori rules,[13,14] intra-chain superexchange *via* oxygen and fluorine atoms with the Fe-(O,F)-Fe angles in the range 89−107° results in FM coupling within chains. These chains are in turn coupled antiferromagnetically to each other by supersuper-exchange *via* phosphate groups (Figure 3c). Finally, the magnetic order between quasi-layers, which are not connected *via* phosphate groups and are separated by the rather long distance of 6.9 Å (Figure 3a) is most likely established with a contribution from long-range dipole−dipole interactions. The structure is not geometrically frustrated (Figure 3c), so the observed moment noncollinearity is likely due to $Fe^{2+}$ anisotropy, which often manifests itself in polyanionic materials.

In summary, we have studied for the first time the magnetic structure and properties of the promising cathode material $Na_2FePO_4F$. The material undergoes a long-range magnetic ordering transition at ∼3.4 K to a noncollinear AFM structure with the moments mainly along the *b*-axis. Our results reconcile previous DFT calculations predicting magnetic ordering[7] and Mössbauer experiments which did not find evidence of magnetic ordering down to 4.2 K.[8]

## ■ ASSOCIATED CONTENT

### Ⓢ Supporting Information

Experimental details of synthesis, magnetic measurements, and Rietveld analysis results. This material is available free of charge via the Internet at http://pubs.acs.org.

## ■ AUTHOR INFORMATION

### Corresponding Author

*Phone: +61-2-9717-9522. Fax: +61-2-9717-3606. E-mail: maxim.avdeev@ansto.gov.au.

### Author Contributions

The manuscript was written through contributions of all authors. All authors have given approval to the final version of the manuscript.

### Notes

The authors declare no competing financial interest.

## ■ ACKNOWLEDGMENTS

C.D.L. acknowledges financial support from the Australian Research Council (DP110102662), and P.B. thanks the Japan Society for the Promotion of Sciences for a JSPS Fellowship at the University of Tokyo.

## ■ REFERENCES

(1) Slater, M. D.; Kim, D.; Lee, E.; Johnson, C. S. *Adv. Funct. Mater.* **2012**, *23*, 947−958.
(2) Padhi, A. K.; Nanjundaswamy, K. S.; Goodenough, J. B. *J. Electrochem. Soc.* **1997**, *144*, 1188−1194.
(3) Ellis, B.; Makahnouk, W.; Makimura, Y.; Toghill, K.; Nazar, L. *Nat. Mater.* **2007**, *6*, 749−753.
(4) Sanz, F.; Parada, C.; Ruiz-Valero, C. *J. Mater. Chem.* **2001**, *11*, 208−211.
(5) Swafford, S. H.; Holt, E. M. *Solid State Sci.* **2002**, *4*, 807−812.
(6) Ellis, B. L.; Makahnouk, W. M.; Rowan-Weetaluktuk, W.; Ryan, D.; Nazar, L. F. *Chem. Mater.* **2009**, *22*, 1059−1070.
(7) Ramzan, M.; Lebegue, S.; Ahuja, R. *Appl. Phys. Lett.* **2009**, *94*, 151904−151904−3.
(8) Lee, I. K.; Shim, I.-B.; Kim, C. S. *J. Appl. Phys.* **2011**, *109*, 07E136.
(9) Masquelier, C.; Croguennec, L. *Chem. Rev.* **2013**, *113*, 6552−6591.
(10) Ramzan, M.; Lebegue, S.; Larsson, P.; Ahuja, R. *J. Appl. Phys.* **2009**, *106*, 043510.
(11) Liang, G.; Park, K.; Li, J.; Benson, R. E.; Vaknin, D.; Markert, J. T.; Croft, M. C. *Phys. Rev. B* **2008**, *77*, 064414.
(12) Rodríguez-Carvajal, J. *Phys. B* **1993**, *192*, 55−69.
(13) Goodenough, J. B. *Magnetism and the Chemical Bond*; Interscience Publishers: New York, 1963; Vol. *1*.
(14) Kanamori, J. *J. Phys. Chem. Solids* **1959**, *10*, 87−98.